Attosecond Electron Dynamics

Matthias F. Kling[1,2] and Marc J.J. Vrakking[1]

[1]FOM Institute for Atomic and Molecular Physics, 1098 SJ Amsterdam, The Netherlands; email: m.vrakking@amolf.nl

[2]Max-Planck Institut für Quantenoptik, D-85748 Garching, Germany

Annu. Rev. Phys. Chem. 2008. 59:463–92

First published online as a Review in Advance on November 21, 2007

The *Annual Review of Physical Chemistry* is online at http://physchem.annualreviews.org

This article's doi: 10.1146/annurev.physchem.59.032607.093532

0066-426X/08/0505-0463$20.00

Key Words

high-harmonic generation, photoionization, ultrafast lasers, interference, laser control, attosecond laser pulses, attosecond streaking spectroscopy, attosecond tunneling

Abstract

We describe the recent emergence of attosecond science, assessing the present state of the art and discussing several recent examples where attosecond electron dynamics has been studied in atomic and molecular systems. After introducing the generation and characterization of attosecond laser pulses, we describe the use of isolated attosecond pulses in a pump-probe experiment revealing the subcycle time dependence of a multiphoton ionization process and an experiment using the interference from a train of attosecond pulses to extract amplitude and phase information for electronic wave functions. We furthermore discuss experiments where ultrashort laser pulses with a reproducible waveform control electron dynamics in the D_2^+ molecular ion on attosecond timescales. Attosecond science is coming of age and presently is reaching a level of maturity and sophistication that allows detailed investigations of the role of multielectron dynamics in physics and chemistry.

1. INTRODUCTION

XUV: extreme ultraviolet radiation

High-harmonic generation (HHG): interaction of an intense laser field, leading to the production of ultrashort XUV pulses

Attosecond laser pulse: laser pulse with a duration of less than 1 fs (1 fs = 10^{-15} s) that can be generated using high-harmonic generation

Processes that lead to the formation of new materials and chemical/biological transformations consist of elementary physical steps that occur on the femtosecond (1 fs = 10^{-15} s), or in some cases the subfemtosecond (attosecond, 1 as = 10^{-18} s), timescale. The natural timescale for the making and breaking of chemical bonds is the vibrational period or, in a language that applies to the condensed phase, the phonon period. These timescales are typically in the femtosecond domain and are consistent with the fact that atoms at thermal velocities ($\sim$1000 m s^{-1}) travel the distance over which a chemical bond changes character ($\sim 10^{-10}$ m) in approximately 100 fs. Electrons are responsible for the creation of the potential energy landscapes that drive atomic motion and adapt on even faster timescales. The typical timescale for electronic motion is the atomic unit of time (1 au = 0.024 fs = 24 as). In the past, direct measurements on these timescales have not been possible. Core-hole clock spectroscopy, in which the rate of an electronic process is compared to the lifetime of a core hole, has been used to determine indirectly that electron transfer from absorbed atoms and molecules to metal surfaces can take place in just 320 as (1).

In the past few decades, the development of laser systems capable of reaching femtosecond pulse durations sparked the widespread use of these systems in studies of time-resolved dynamics, leading to significant advances in our understanding of intramolecular processes, chemical bond breaking and bond formation, and the interaction of photoactivated molecules with their environment. In 1999 this work culminated in the Nobel Prize in Chemistry for Zewail (2). Experiments on time-resolved electron dynamics have thus far been sparse, with the exception of the physics and chemistry of Rydberg states (3), where electronic motion is slowed down because in highly excited states the electron only weakly interacts with the positive ion core. In Rydberg atoms and molecules, the relevant timescales for electronic motion, as dictated by the inverse of the available energy-level splittings, can be in the picosecond domain (4) or even in the nanosecond domain. In the latter case, one can use nonoptical methods to perform time-resolved experiments (5, 6).

The quest to probe atomic and electronic dynamics on ever shorter timescales inevitably leads to the use of extreme ultraviolet (XUV)/X-ray radiation. Because the duration of a single optical period is 2–3 fs for visible light, laser pulses in the visible are necessarily approximately 4 fs or longer (7, 8). To synthesize shorter pulses, one must employ laser fields containing significantly higher frequencies extending into the XUV/X-ray regime (9). High-harmonic generation (HHG) and stimulated Raman scattering are two techniques that generate frequency components over a wide range (10–13). In HHG, the highly nonperturbative interaction of an intense femtosecond laser with an atomic or molecular medium generates new frequencies at photon energies up to a few kilo–electron volts (14). In a major breakthrough in 2001, two teams independently demonstrated that HHG leads to the emission of ultrashort light bursts, lasting just a few hundred attoseconds (15, 16). These results sparked the emergence of the new field of attosecond science, which is now rapidly gaining ground worldwide and is driven by the notion that the availability of attosecond laser pulses may allow one to perform attosecond pump-probe experiments, in which a first attosecond pump pulse electronically excites an atomic, molecular, or condensed

phase system of interest, thereby initiating an ultrafast electronic process, and in which a second, time-delayed attosecond probe pulse extracts a signal from the system containing information about the time evolution that has taken place.

IR: infrared

The purpose of the present review is to describe the recent emergence of attosecond science, to assess the present state of the art, and to discuss several recent examples applying attosecond pulses to study atomic and molecular electron dynamics. A number of recent reviews have already discussed the physics of generating and characterizing attosecond laser pulses in considerable detail (17–21), and Corkum et al. (22) gave an earlier contribution to this series in 1997, predicting the advent of attosecond pulses. Here we emphasize the emerging applications of attosecond science, which is presently reaching a level of maturity and sophistication that allows the investigation of hitherto inaccessible physics and chemistry.

1. HIGH-HARMONIC GENERATION AND THE EMERGENCE OF ATTOSECOND LASER PULSES

1.1. High-Harmonic Generation and the Formation of Attosecond Pulse Trains

In HHG an atomic or molecular medium is exposed to an intense femtosecond laser that typically operates in the near-infrared (near-IR) part of the spectrum. Ionization by this laser ejects electrons that are accelerated in the oscillatory electric field of the laser (see **Figure 1**). A finite fraction of the electrons recollides and recombines with

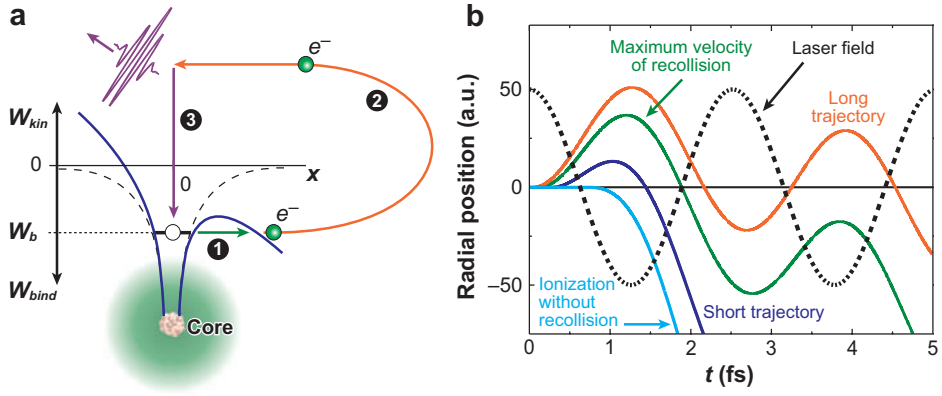

Figure 1

(*a*) Illustration of the three-step mechanism of high-harmonic generation (HHG) that leads to the creation of attosecond pulses. (*b*) Trajectories of the electrons involved in HHG as a function of the time (phase of the driving field) when the ionization occurs. When the electron ionizes at a phase of +0.3 radians with respect the laser field maximum, the highest extreme ultraviolet (XUV) photon energy ($h\nu = IP_{target} + 3.17\ U_p$) is produced. Electrons emitted after and before this time follow so-called short and long trajectories, respectively. The dependence of the XUV photon energy on the instance of recombination implies that the attosecond pulses are chirped.

their parent ion, producing an XUV/soft X-ray photon (23, 24). The highly nonlinear dependence of the initial ionization event on the electric field of the femtosecond laser constrains the electron ejection to short time intervals near the maximum of the optical cycle. After acceleration, during which the electrons follow well-defined trajectories, this leads to a situation in which XUV/soft X-ray photons are produced in short bursts with a duration that is a small fraction of the optical cycle of the driver laser (2.7 fs in the case of the popular Ti:sapphire laser). The formation of an attosecond pulse takes place during every optical half-cycle when the probability of electron ejection is sufficiently high and the femtosecond laser is linearly polarized. Therefore, attosecond pulses generally are produced in a train, with two pulses occurring per half-cycle of the driver laser (15, 25, 26). Interference between these XUV bursts gives the radiation its characteristic spectral signature, with harmonics produced at odd multiples of the frequency of the driver laser for rare-gas atoms. Consequently, the technique is commonly referred to as high-order harmonic generation (27). In HHG an XUV spectrum is generated that consists of three distinct regions: (*a*) a perturbative region (in which the XUV photon energy is below the ionization potential of the target gas), (*b*) a plateau region (in which the yield of the harmonics is approximately constant), and (*c*) a cutoff region at high energy (in which the intensity of the individual harmonics rapidly decreases). The location of the cutoff depends on the ionization potential of the target and the intensity of the laser used (23) and is given by

$$E_{cutoff} = IP_{target} + 3.17\,U_p, \tag{1}$$

where IP_{target} is the ionization potential, and $U_p = I/4\omega^2$ is the ponderomotive energy at the intensity I and frequency ω of the laser.

1.2. Isolated Attosecond Pulses Using Cutoff Harmonics

Attosecond pulse trains, although suitable for a number of specialized applications, are not ideal for attosecond pump–attosecond probe experiments as described above because there is an ambiguity in the time delay between the pump and probe photoabsorption. Therefore, researchers have directed much effort at producing isolated attosecond pulses. This was achieved by restricting the number of driver laser cycles that allow for the ejection of electrons in combination with either spectral or temporal selection. Investigators have implemented successfully both approaches. Krausz and coworkers (16, 28–31) used extremely short, so-called few-cycle laser pulses, in which the electric field amplitude differs considerably from one half-cycle to the next. For a suitable waveform of the pulses, the highest-energy XUV photons are produced only during the most intense half-cycle of the driver laser. Selection of these highest-energy XUV photons (the cutoff harmonics) consequently allows for the generation of an isolated attosecond pulse (32). To produce the isolated attosecond pulse reliably and reproducibly, it is necessary that the electric field waveform of the laser is stable from pulse to pulse (29). The electric field of a laser pulse can be expressed as

$$E_L(t) = E_0(t)\,\cos(\omega_L t + \varphi), \tag{2}$$

where $E_0(t)$ is a slowly varying amplitude function; ω_L is the laser carrier frequency (which may also be slowly varying); and φ is the so-called carrier-envelope phase (CEP), which describes the offset of the laser's electric field maxima with respect to the maximum in the envelope function. Stabilization of the CEP requires matching the phase and group velocities of the propagating laser pulses (33). In the past few years, the development of CEP-stable laser systems has revolutionized frequency metrology, and in the optical domain frequency measurements with a fractional uncertainty of 10^{-15} have become a reality (34). In 2005 Hänsch (35) and Hall (36) received the Nobel Prize in Physics for their contributions to the development of the optical frequency comb technique. The crucial impact of CEP stabilization on attosecond science is that it has paved the way to stable and reproducible production of isolated attosecond pulses (29). Owing to the importance of CEP stabilization, there is currently a lot of activity aimed at the development of CEP diagnostics (37–41). As an example, Haworth et al. (41) have shown recently that the observation of half-cycle cutoffs in high-harmonic spectra is a suitable method for determining the CEP.

Carrier-envelope phase (CEP): phase φ that describes the offset of the electric field oscillations with respect to the maximum of the envelope of a (short) laser pulse

1.3. Isolated Attosecond Pulses Using Polarization Gating

Although the use of cutoff harmonics allows the generation of isolated attosecond pulses, a disadvantage of the technique is that it requires few-cycle driver laser pulses and the cutoff region of the high-harmonic spectrum, both of which severely limit the efficiency. Whereas using high-energy driver lasers can lead to the production of attosecond pulse trains with as many as 10^{11} photons per pulse (42), isolated attosecond pulse production using cutoff harmonics thus far remains approximately five orders of magnitude below these values. Following an idea originally put forward by Corkum et al. (43) in 1994, researchers therefore have pursued harmonic generation from polarization gated driver pulses. Electron recollision is an important step in harmonic generation and requires the laser polarization to be sufficiently linear. In polarization gating, the pulses are shaped to exhibit linear polarization during just a single cycle and elliptical/circular polarization for all other cycles, restricting the harmonic generation to a single cycle. Whereas Corkum et al. (43) proposed accomplishing polarization gating using two orthogonally polarized laser pulses centered around a different carrier frequency, the first experimental implementation by Kovacev et al. (44) made use of birefringent optics. They used a birefringent delay plate that splits the incident beam into two orthogonally polarized pulses that are delayed with respect to each other, followed by a $\lambda/4$ plate that converts the circular polarization in the overlap region of the two pulses into a linear polarization, while converting the linearly polarized trailing and falling edge (where the two pulses no longer overlap) into circularly/elliptically polarized light. Using a polarization gate allows the generation of attosecond pulses in the plateau region of harmonic generation, where the conversion efficiency is high. It thereby offers the potential for more intense and shorter attosecond pulses. One initial demonstration of polarization gating showed a reduction of the length of an attosecond pulse train from 38 to 18 fs (45). An implementation of polarization gating using a few-cycle driver laser (in combination with a suitable dispersive filter) by

Sansone et al. (46, 47) led to the current world record in accomplished pulse duration (130 as).

1.4. Ongoing Developments Toward More Intense Attosecond Pulses

A disadvantage of the polarization gating methods used so far is that the most intense half-cycle of the laser field is not used. Rather, the attosecond pulses are produced on the falling respective trailing edge of two overlapping time-delayed pulses. Consequently, when applied toward the production of isolated attosecond pulses, the pulse intensities have remained low. The generation of isolated attosecond pulses that are intense enough to perform attosecond pump–attosecond probe experiments therefore remains an important challenge for the coming years. Approaches proposed toward the development of more intense attosecond pulses include the generation of harmonics on surfaces (48, 49) and the use of polarization gates that do not require few-cycle laser pulses. In surface harmonic generation, a solid target is irradiated at an intensity of $\geq 10^{18}$ W cm^{-2}, leading to the formation of an overdense plasma. Attosecond pulses are then produced as a result of the compression of laser electric field oscillations upon reflection off the oscillating plasma mirror produced by the intense femtosecond laser and by radiation from electrons oscillating in the plasma. Recent results on surface harmonic generation include the generation of harmonics up to 700 eV using the VULCAN laser (50) and a characterization of the relative importance of the oscillating mirror model and the coherent plasma oscillations (49). A temporal characterization has not been performed. Tzallas et al. (51) recently proposed an interferometric polarization gating method that extends the generation of isolated attosecond pulses by means of polarization gating to many-cycle driver lasers, which in principle can reach terawatt levels.

1.5. Attosecond Pulse Generation Using Two-Color Fields

As discussed above, the original proposal for polarization gating was based on the use of a two-color laser field (43). Recently, there has been increased activity on two-color harmonic generation, using copolarized and orthogonally polarized pairs of harmonic and nonharmonic beams. Inspired by an experiment by Zamith et al. (52), which demonstrated the control of atomic ionization under the influence of a two-color (copolarized) radio-frequency laser field, Siedschlag et al. (53) showed that isolated attosecond pulses could be formed from many-cycle ($\tau_{FWHM} \sim 19$ fs) driver pulses by a suitable choice of the two laser frequencies. The tuning of the frequencies affects both the ionization and the recollision dynamics during the harmonic generation process. Although in this work the laser frequencies were incommensurate (i.e., not a harmonic of each other), Pfeifer et al. (54, 55) subsequently analyzed attosecond pulse generation by a superposition of two copolarized harmonic fields. Similar to the method used by Krausz and coworkers (16, 28–30), this two-color approach utilizes cutoff harmonics, although with significantly reduced requirements on the length of the driver laser pulse. Mauritsson et al. (56) have studied HHG using the superposition of a fundamental and second harmonic laser field, aiming to produce attosecond pulse

trains with one instead of two pulses per optical cycle. Application of this technique may resemble the use of an isolated pulse to the extent that the electron dynamics under investigation occurs with the periodicity of the driver laser (as is the case in many strong-field problems). An interesting aspect of this work is that all pulses have the same CEP in such a train. Hence, when the intensity of the attosecond pulse trains can be increased to the point that nonlinear absorption becomes dominant, the CEP may become available as a parameter that can be used to control dynamics, similar to the way that this has been possible in the optical domain (57, 58).

1.6. High-Harmonic Generation as a Tool for Obtaining Structural and Dynamical Information

In addition to the use of HHG as a tool for producing attosecond light pulses, the process itself has also been developed into a tool for obtaining structural and dynamical information (59). Because we can view HHG as emission from an oscillating dipole that results from interference of the recollision electron with the ground-state wave function, the structure of electronic orbitals is imprinted on the HHG spectrum. In a pioneering experiment, Itatani et al. (60) showed that the ground-state orbital of the N_2 molecule can be retrieved by measuring an HHG spectrum at a range of alignment angles of the molecular frame with respect to the polarization of the driving laser. One can vary the alignment angle by making use of the fact that in a strong laser field, molecules can be polarized and dynamically aligned along a chosen axis using a suitable pump laser pulse (61).

The HHG process provides access to the molecular structure as well. Following theoretical predictions by Lein et al. (62), Kanai et al. (63) observed quantum interference in HHG where constructive and destructive interference occurred for selected harmonics subject to a Bragg condition for the returning electron. One can use the harmonic order where the constructive or destructive interference occurs to deduce the internuclear distances in the molecule. Electron diffraction in the frame of a molecular ion can also be observed by means of a measurement of the angular distribution of emitted or rescattered photoelectrons (64, 65). When measuring rescattered photoelectrons, in the latter case, one exploits the fact that HHG can be viewed as an electron-ion recollision process where the ion is exposed to an electron current density that reaches 8×10^{11} A cm^{-2} (66). The arrival of this recollision electron at the positive ion core occurs predominantly during a small fraction of the optical cycle of the driver laser, implying that the electron probes the ion with attosecond time resolution. In experiments on D_2^+ dissociation, one could thus map the first few femtoseconds of the molecular dissociation by using a wavelength-tunable ionization laser, where variation of the wavelength translates into a variable recollision time (67). Exploiting the known relation between the recollision time and the energy of the recollision electron, Baker and coworkers (68) recently extended this approach and tracked the initial stages of the dissociation of H_2^+ into $H^+ + H$ using a single driver laser wavelength. The elongation of the internuclear bond leads to a reduction of the high-harmonic yield, which depends on the precise time at which the harmonics are produced. Observation of this reduction as function of the

harmonic order therefore allows one to derive the internuclear distance as a function of time.

RABBITT: reconstruction of attosecond beating by interference of two-photon transitions

Although in all these experiments the nuclear and electronic dynamics were induced by the same laser pulse, one can also apply recollision-based probes of electronic and nuclear structure and dynamics to resolve processes induced by another laser pulse. Wagner and coworkers (69) performed stimulated Raman excitation on SF_6 molecules and observed time-dependent oscillations and relaxation in the high-harmonic yield that reflected the induced nuclear motion. In the coming years, we may expect considerable efforts in this direction. Pump-probe experiments likely will be performed in which a pump pulse initiates electronic or structural dynamics in a molecule, which is subsequently probed by time-delayed HHG monitoring the time-dependent electronic and nuclear configuration of the molecule.

2. CHARACTERIZATION OF ATTOSECOND LASER PULSES

In the years since the initial reports on the production of attosecond laser pulses, investigators have devoted significant effort toward the development of techniques for the complete characterization of the radiation. Initially, these developments proceeded independently along a number of distinct paths. More recently, the commonality between many of these methods has been appreciated (70).

2.1. Characterization of Attosecond Pulse Trains Using the RABBITT Technique

The first experiment on the characterization of attosecond laser pulses was the characterization of a train of pulses by means of the RABBITT (reconstruction of attosecond beating by interference of two-photon transitions) technique introduced by Paul et al. (15). Utilizing the alternate description of ultrashort pulses through their time-dependent electric field $E(t)$ or through the complex spectral amplitude $E(\omega)$, this technique relies on reconstructing the envelope of $E(t)$ by measuring the harmonic intensity spectrum ($|E(\omega)|^2$) and the relative phase of a comb of adjacent harmonics. These parameters are obtained in an interference experiment in which the harmonic laser ionizes atoms in the presence of a moderately intense (10^{11}–10^{12} W cm^{-2}) replica of the IR driving field used to produce the harmonic radiation. The photoelectron spectrum then contains side bands at energies corresponding to the absorption of an even number of IR photons, owing to absorption of one of the harmonics accompanied by the absorption or stimulated emission of an IR photon (see inset in **Figure 2*a***). Each side band q thus contains interfering contributions from the two neighboring odd harmonics $(q-1)\omega$ and $(q+1)\omega$. Observation of the yield of the side bands and/or their angular distribution allows one to extract the relative phase of these two harmonics. Concatenation of these phases for all harmonics then allows one to reconstruct the XUV pulse envelope.

Figure 2*a* shows an experimental setup used by Aseyev et al. (25), and **Figure 2*b*** shows the result for three RABBITT experiments performed using this setup, generating high harmonics in Xe, Kr, and Ar. Clearly, an attosecond pulse train is produced

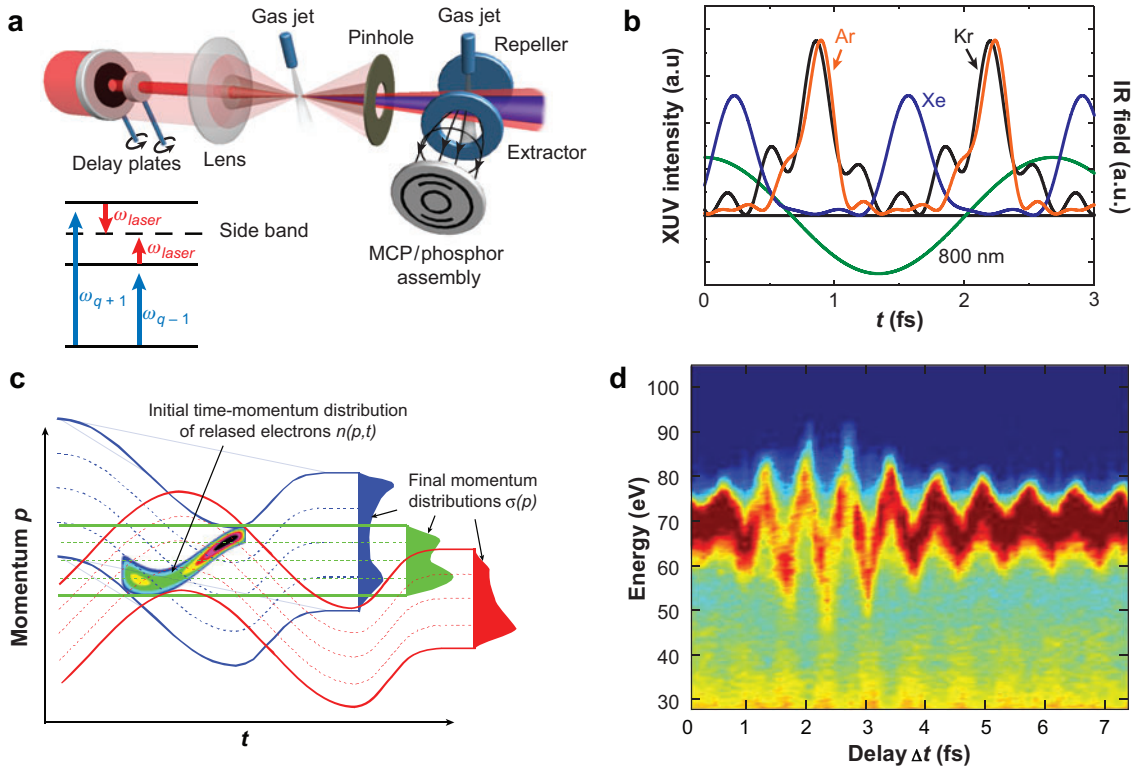

Figure 2

(*a*) Experimental setup for a RABBITT measurement, in which side bands involving adjacent harmonics are measured to determine their phase relationship. (*b*) Reconstructed attosecond pulse trains, characterized by means of the RABBITT technique (25). (*c*) The principle of an attosecond streak camera measurement, in which a kinetic energy measurement is performed that contains information on the attosecond pulse duration, the shape of the IR streaking field, and the (non)instantaneous response of the ionized target (30). (*d*) Streak camera measurement obtained by ionizing Ne atoms with an isolated attosecond laser pulse in the presence of a strong IR streaking field. The measurement was performed by means of angle- and energy-resolved photoelectron detection using a velocity-map imaging spectrometer. MCP, microchannel plate.

in each case, with a minimum pulse duration of approximately 250 as. Remarkably, these measurements show that the attosecond pulse train generated in Xe is time-shifted (by approximately one-quarter of an optical period) with respect to the ones generated in Kr and Ar. This violates the semiclassical description of HHG, which predicts that ionization occurs near the maximum of the electric field of the driver laser and is accompanied by the formation of an attosecond pulse near the zero-crossing of the electric field, approximately one-quarter of a cycle later (23). This deviation may result from differences in the ionization of the medium in question (predominance of field versus multiphoton ionization) or differences in phase-matching conditions,

including the dominance of short over long trajectories. In the case of Ar, Dinu et al. (71) measured the occurrence of the attosecond pulses near a zero crossing of the driving field. Mairesse et al. (26) used the RABBITT technique to determine the chirp of the harmonics over a wide bandwidth and concluded that—in agreement with semiclassical predictions—the attosecond pulses are produced with a chirp resulting from the variation of the recollision electron's kinetic energy as a function of time (within the optical cycle of the driver laser). By choosing the optimum spectral bandwidth, they produced a train of 130-as pulses in Ne (26, 72).

2.2. Characterization of Isolated Attosecond Pulses Using an Attosecond Streak Camera

Whereas RABBITT relies on the use of an IR dressing field at a perturbative intensity, the attosecond streaking technique (see **Figure 2*c***) pioneered by Krausz and coworkers relies on the use of an intense (10^{13}–10^{14} W cm^{-2}) IR laser field that exchanges many photons with the electron after it has been set free in the continuum by the attosecond pulse(s) (73, 74). This exchange is understood most conveniently in terms of the acceleration and the velocity change that the electron undergoes in the presence of the external field. The velocity of the electron can be written as

$$v(t) = -\int (e/m)E_L(t)\,dt + [v_0 + (e/m)A_L(t_i)] = -(e/m)A_L(t) + [v_0 + (e/m)A_L(t_i)], \quad (3)$$

where $E_L(t)$ and $A_L(t)$ are the electric field and the vector potential of the IR laser field used, respectively; v_0 and $v(t)$ are the initial electron velocity at release time t_i and at a later time $t > t_i$, respectively; and e and m are the electron charge and mass, respectively. The term $-(e/m)A_L(t)$ is the quiver energy of the electron, which goes to zero when the laser pulse is over. The time of creation of the electron in the continuum (t_i) maps onto a velocity displacement that depends on the vector potential of the IR laser, explaining why this technique was named attosecond streak camera (73). Using the attosecond streak camera, Krausz and coworkers demonstrated the production of isolated attosecond laser pulses with a duration of 650 (16) and more recently 170 as (75). Attosecond streaking measurements are influenced by (*a*) the duration of the attosecond pulse, (*b*) the shape of the IR streaking field, and (*c*) the temporal response of the medium, which may or may not be instantaneous (28, 76). Hence, if two of the three are known, the third can be revealed by the measurement. Drescher et al. (77) analyzed the influence of a noninstantaneous response of the medium on the measured energy distributions (see below), whereas Goulielmakis et al. (78) characterized experimentally the shape of the IR streaking field. **Figure 2*d*** illustrates a recent example of an attosecond streaking measurement employing a velocity-map imaging spectrometer (79, 80). Using the attosecond streaking technique, Sansone and colleagues (46, 47) determined the temporal structure of isolated attosecond pulses generated by polarization gating, leading to the shortest experimentally demonstrated pulse duration of 130 as.

2.3. Self-Referencing Attosecond Pulse Characterization Methods

Both RABBITT and the attosecond streak camera are methods characterizing attosecond laser pulses by using IR light. Self-referencing pulse characterization methods based on use of the XUV light alone have been considerably more challenging to implement. In the optical domain, the most common method for the characterization of short pulses is an intensity autocorrelation, in which a nonlinear response $S_{NL}(\delta t)$ is measured for two time-delayed replicas of the pulse to be characterized:

$$S_{NL}(\delta t) = \int I(t)\, I(t + \delta t)\, dt. \quad (4)$$

Velocity-map imaging spectrometer: two-dimensional detector that records the velocity distribution of ions or electrons formed in a laser ionization experiment

SPIDER: spectral interferometry for direct electric field reconstruction

Owing to the limited intensity available in presently existing attosecond sources, implementing autocorrelation measurements is challenging. Tzallas et al. (81) performed autocorrelation measurements for an attosecond pulse train by nonresonant two-photon ionization in He and observed attosecond light bunching with an inferred 780-as duration of individual pulses in the train. The longer pulse duration obtained as compared to the results of the above-mentioned RABBITT measurements was explained in terms of spatial variations in the temporal width of the XUV radiation (82). Sekikawa et al. (83) used 400-nm driver pulses to generate the ninth harmonic (27 eV) and measured an intensity autocorrelation revealing a pulse duration of 950 as. More recently, these experiments were extended into frequency-resolved optical gating measurements, in which the two-photon photoelectron spectrum was measured as a function of the delay between two XUV pulse replicas, thereby allowing a determination of the spectral phase of the XUV pulse (84, 85). Nabekawa et al. (86) reported recently a mode-resolved autocorrelation technique in which they measured the two-photon photoelectron spectrum for Ar ionization by a pair of attosecond pulse trains, allowing the determination of the chirp in the attosecond pulse train. From an interferometric autocorrelation using the detection of N^+ ions resulting from two-photon dissociative ionization of N_2, these authors concluded that their experiment produced a train of 320-as-long pulses (87).

Varju et al. (88, 89) studied the relation between the chirp of individual harmonics and the chirp of individual attosecond pulses in a pulse train. Using an adiabatic expansion of the spectral phase of the XUV light (as a function of time and harmonic order), these authors determined pulse-to-pulse variations along the train including the timing and the chirp of the attosecond pulses. Queré et al. (91) and Cormier et al. (92) pursued the extension of SPIDER (spectral interferometry for direct electric field reconstruction) (90) methods to attosecond pulse characterization. The first experimental demonstration of SPIDER in the XUV regime was performed by Mairesse et al. (93).

Dudovich et al. (94) recently published a new method for the characterization of attosecond pulse trains where the characterization already takes place in the generating medium. HHG was performed in which the fundamental driving laser field was supplemented by a small (~1%) amount of second harmonic light that created an imbalance between electron trajectories during successive half-cycles of the driver laser pulse. This imbalance leads to the formation of even harmonics, which one can

monitor as a function of the phase difference between the fundamental and second harmonic laser field, thereby revealing the emission time of the harmonic and—in principle—allowing a reconstruction of the temporal structure of the attosecond pulse train.

3. THE DESIGN OF ATTOSECOND PUMP-PROBE EXPERIMENTS

The holy grail of attosecond science research is to perform experiments where an attosecond XUV pump pulse initiates electron dynamics that is subsequently probed by an attosecond XUV probe pulse, with both pulses having a duration that is short compared to the typical timescale of the electron dynamics under investigation. For example, Hu & Collins (95) recently calculated two-color ionization of He using a sequence of two ultrashort XUV pulses, namely a 1.5-fs, 23.7-eV pump pulse and a 250-as, 90-eV probe pulse. An evaluation of the total double ionization cross section and the energy sharing between the two emitted electrons revealed clearly the motion of the electronic wave packet produced by the pump pulse. Yudin et al. (96) analyzed the ionization of a set of coherently coupled states using an attosecond pulse and concluded that the angle-resolved photoelectron spectrum contains detailed information about the time dependence of the electronic wave packet prior to ionization.

3.1. Present Status of Attosecond Pump-Probe Capabilities

XUV pump–XUV probe experiments have not been performed thus far. Although a few teams have observed two-photon absorption in experiments characterizing attosecond pulse trains by means of autocorrelation (81, 83, 85–87), experiments with isolated attosecond pulses have thus far been limited to single-photon absorption. In practice this has meant that pump-probe experiments aimed at investigating attosecond-timescale electron dynamics rely on using the highly nonlinear interaction of an IR laser as an ultrafast subcycle gate that either initiates the electron dynamics or probes the electron dynamics on attosecond timescales. In the long run, this is undesirable because this inevitably restricts the use of attosecond techniques to experiments where the intense field interaction of the IR laser cannot be neglected and in fact often becomes the objective of the experiment itself.

Two types of experiments have thus far been developed, where the role of the IR laser field has been to accelerate electrons produced by the attosecond laser (73, 74, 77) or to ionize electrons from excited states resulting from the interaction with the attosecond laser (97). The attosecond streak camera mentioned above represents an example of the former case (30). Below we give two examples illustrating the use of ponderomotive acceleration (streaking) and ionization by a strong IR field as methods for obtaining an attosecond response, at the same time pointing out some of the possibilities provided by the availability of isolated attosecond pulses and attosecond pulse trains.

4. EXAMPLE 1: ISOLATED ATTOSECOND LASER PULSES AND THE USE OF SUBCYCLE IONIZATION

A limited number of experiments exist that use isolated attosecond pulses to elucidate atomic or molecular electron dynamics. Only two concrete examples exist, both performed by Krausz and coworkers (77, 97). At the same time, these experiments are examples of the two ways that the IR field can be employed to obtain an attosecond response. The first experiment used streaking to determine the lifetime toward Auger decay of Kr atoms (77). A sample of Kr atoms was ionized by an isolated 250-as pulse centered around 90 eV in the presence of a strong IR field. The removal of an M-shell electron from the atom was accompanied by an MNN Auger decay. The authors determined the rate of this Auger decay by monitoring the ejection of the emitted Auger electrons into the IR streaking field (which changed their velocity) and found the Auger lifetime to be 7.9 fs. By contrast, the second experiment exploited the subcycle time dependence of strong-field ionization rates to measure electron dynamics in bound states of the Xe and Ne atom (97). **Figure 3** illustrates some of these results (see below).

The strong-field ionization process shown in **Figure 1** forms the basis of the HHG process (23) and is one of the two ways that strong-field ionization processes are described. Depending on the value of the so-called Keldysh parameter [$\gamma = \sqrt{(IP/2U_P)}$], ionization is described alternatively in terms of a multiphoton

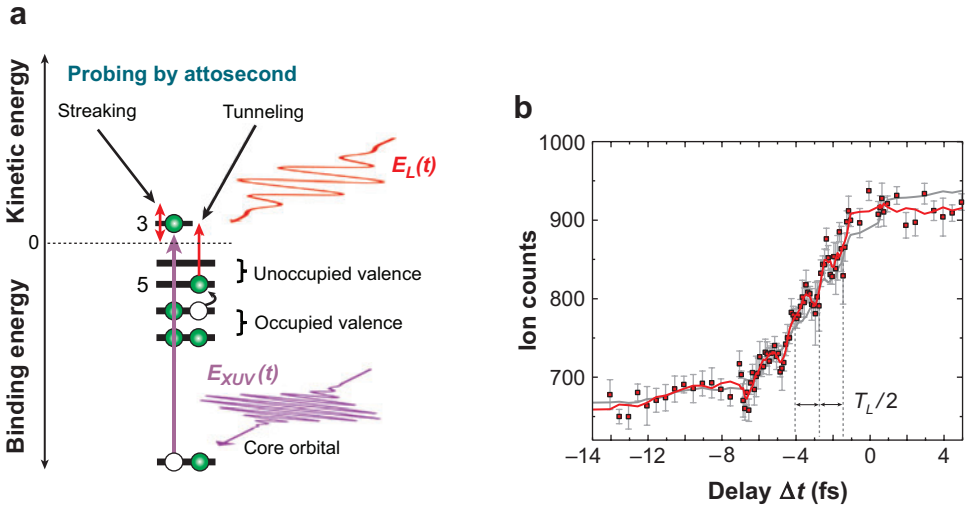

Figure 3

(*a*) Principle of Krausz and coworker's (97) experiment measuring the subcycle time dependence of strong-field ionization. An isolated attosecond XUV pulse removes a core electron and leads to shake up of a second electron to an excited state, from which it can be ionized by an intense IR pulse. (*b*) Dependence of the Ne^{2+} yield as a function of the delay between the isolated attosecond pulse and the few-cycle IR pulse, revealing that the ionization by the IR laser occurs in a series of steps, with two steps occurring per optical cycle.

ionization or a tunneling/over-the-barrier ionization process (98). In the multiphoton ionization picture ($\gamma \gg 1$), one considers that overcoming the ionization potential *IP* requires the absorption of at least $IP/(\hbar\omega)$ photons. For small frequencies ω, this involves the absorption of multiple photons and thus requires an intense laser. In the tunneling/over-the-barrier picture ($\gamma \ll 1$), one considers the distortion of the Coulomb potential caused by the laser's electric field. Ionization becomes possible when the barrier in the Coulomb plus laser field potential (at an energy $-2\sqrt{E_L}$, where E_L is—as above—the laser electric field strength) becomes comparable to the electron's binding energy. Interestingly, whereas tunneling/over-the-barrier ionization occurs with a rate that strongly varies within the optical cycle (and peaks when the magnitude of the electric field reaches a maximum), multiphoton ionization is expected to occur throughout the optical cycle (99). Hence, on attosecond timescales, the two mechanisms are expected to be distinguishable.

Krausz and coworkers' (97) accessed experimentally the timescale for strong-field ionization. Ne atoms were ionized by an isolated attosecond laser pulse centered around 90 eV, in the presence of a strong laser field ($I \approx 7 \times 10^{13}$ W cm^{-2}). A small fraction of the ionization events leading to the production of Ne^+ was accompanied by excitation (shake up) of the Ne^+ ion to excited states, enabling the ion to be further ionized by the IR laser field (to Ne^{2+}). Importantly, varying the time delay between the isolated attosecond pulse and the few-cycle IR laser allowed a choice of the number of laser cycles that could contribute to the formation of Ne^{2+} and thus allowed the authors to distinguish the contribution from individual cycles (as seen in **Figure 3**). In this fashion, the experiment provided clear evidence for the existence of subcycle variations in the ionization rate.

Simulations of the experiments were performed both by using Yudin & Ivanov's (99) nonadiabatic tunneling theory and by numerically solving the time-dependent Schrödinger equation (100). In the latter case, the shake-up states were assumed to be formed by resonant excitation starting from the Ne^+ $2s/2p$ orbital. Interestingly, calculations revealed that over the entire range of intensities that could be accessed ($\gamma = 1$–8, i.e., deeply penetrating what would ordinarily be considered the multiphoton regime), subcycle variations in the ionization rates remained observable. The ionization rates calculated using Yudin & Ivanov's nonadiabatic tunneling theory showed remarkable agreement with the time-dependent Schrödinger equation results, suggesting that tunneling remains important at intensities more commonly associated with the multiphoton regime (100).

5. EXAMPLE 2: ATTOSECOND PULSE TRAINS AND THE USE OF PONDEROMOTIVE ACCELERATION

Ponderomotive acceleration was the basis of Krausz and coworkers' (16) first characterization of isolated attosecond pulses. At first sight, ponderomotive acceleration is not a technique that lends itself toward the characterization of attosecond pulse trains because ponderomotive streaking leads to the overlap (in momentum space) of electrons produced by a wide range of harmonics. Nevertheless, the use of ponderomotive streaking in combination with the use of attosecond pulse trains allows

the development of a new type of electron wave-packet interferometry that offers the potential for complete (amplitude and phase) characterization of electronic wave packets (101, 102). Characterizing electronic wave functions has become a prominent topic in attosecond science, following Itatani et al.'s (60) pioneering experiment (see Section 1). The use of an attosecond pulse train allows the preparation of a series of wave-function replicas in the continuum. Under the influence of a strong IR driving field, one can modify the phase and/or velocity of these continuum electrons, allowing for the observation of interference patterns that contain information about the IR driving field and/or the wave-function replicas. In the latter case, we can view the experiment as a self-referencing analog of Itatani et al.'s (60) experiment.

5.1. Attosecond Electron Wave-Packet Interferometry

Figure 4 illustrates the concept of attosecond electron wave-packet interferometry, as the technique has been called, in more detail. If an isolated attosecond pulse is used to eject an electron in the continuum, it exhibits a characteristic momentum distribution (**Figure 4*a***) that can be altered by streaking in the presence of a strong IR field (**Figure 4*b***). If one instead uses a train of attosecond pulses, multiple electron wave packets are produced in the continuum, and these electrons are subsequently accelerated (**Figure 4*c*,*d***). The velocity change is simply equal to the vector potential $A_L(\tau)$ at the time of the ionization process (see Equation 2). In the limit of a train of infinitely short attosecond pulses and a long IR pulse [i.e., $A_L(t) = A_0 \sin(\omega t)$], the phase difference at final momentum p between two electron wave packets that are ionized at times $\tau' = (k+1)\pi/\omega$ and $\tau = k\pi/\omega$ [by the $(k+1)$-th and k-th attosecond pulse, respectively] is given by

$$\Delta\Phi_k = -W\frac{\pi}{\hbar\omega} - (-1)^k \frac{2eA_0 p_y}{m\hbar\omega}\cos(\omega\tau) + \Delta\phi_k + \pi, \tag{5}$$

where

$$\Delta\phi_k = \phi[p + (-1)^{k+1} e A_L(\tau)] - \phi[p + (-1)^k e A_L(\tau)] \tag{6}$$

and $W = p^2/(2m) + IP + U_p$ (103). We can consider two limiting cases:

1. If the ionization occurs at a maximum of the electric field of the laser [i.e., at a zero of $A_L(\tau)$], then the electrons undergo a phase shift $\Delta\phi_k$ under the influence of the IR field, maintaining their initial velocity (see **Figure 4*c***). In this case the interferogram is determined by the phase evolution under the influence of the IR field and can be used to characterize this field, in a manner complementary to Goulielmakis et al.'s (78) streak camera determination of the field.
2. If the ionization occurs at a zero crossing of the laser's electric field [i.e., at a maximum of $|A_L(\tau)|$], then the electrons undergo a velocity change under the influence of the IR field, which has the opposite sign for consecutive pulses (see **Figure 4*d***). In momentum space, one can then measure an interferogram in which at final momentum p, momentum components initially ejected at momentum $p - A_L$ and $p + A_L$ interfere with each other. We can view the experiment as an interferometric technique that compares the phase for two

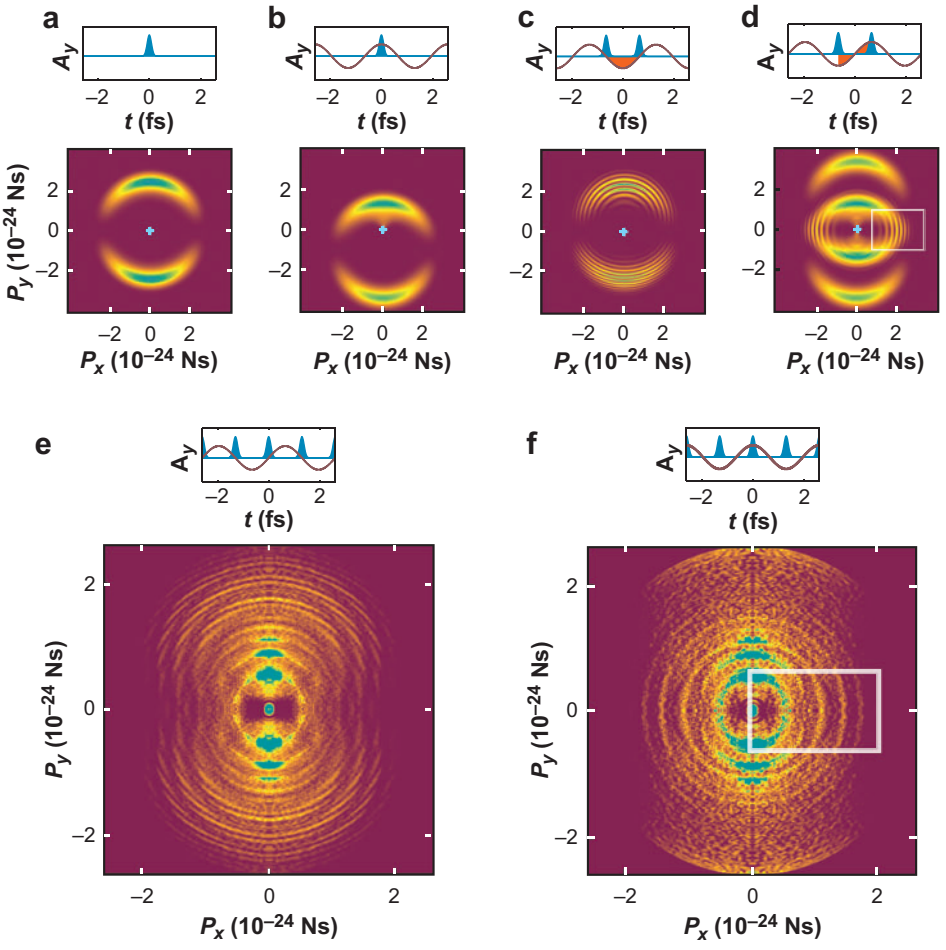

Figure 4

Principle of the attosecond electron wave-packet interferometry experiment. The phase and/or velocity distribution of electrons ionized using (*a*) a single attosecond pulse alone and (*b*) within a moderately strong IR field. (*c*) When the pulses in an attosecond pulse train coincide with zero crossings of the vector potential $A_L(t)$, interferograms are measured that are due to an acquired phase difference. (*d*) When the attosecond pulses coincide with the maxima/minima of the vector potential $A_L(t)$, the electrons undergo a velocity displacement, which has the opposite sign for consecutive attosecond pulses. (*e*,*f*) Experimental velocity-map images obtained using a long train of attosecond pulses synchronized to the zero crossings respective to the maxima/minima of the vector potential (102). Figure courtesy of T. Remetter.

different values of the initial momentum. As such, the technique has strong similarities with the SPIDER technique for the reconstruction of optical fields, in which the phase of different frequency components within a laser bandwidth is compared to arrive at a complete reconstruction of the spectral phase function (90). Of course, whereas the phase function $\phi(\omega)$ of an optical light field is a

one-dimensional function, the phase function of an electronic wave function is generally a three-dimensional object. This implies that full reconstruction of an electronic wave function requires ponderomotive streaking in multiple directions.

5.2. First Demonstration of Attosecond Electron Wave-Packet Interferometry

Remetter et al. (102) reported a practical realization of the attosecond electron wavepacket interferometry described above. The authors generated a train of attosecond pulses using HHG in Ar and combined the train with a colinearly copropagating IR beam. The two beams were focused (using a toroidal mirror) into a velocity-map imaging spectrometer (79). Photoelectrons resulting from atomic ionization at the crossing point between the two laser beams and an Ar atomic beam were accelerated toward a dual microchannel plate assembly, followed by a phosphor screen and a camera system that recorded the position of electron impacts. Two sample images, recorded for $A_L(\tau) = 0$ and $A_L(\tau) = A_{max}$, are shown in **Figure 4*e*,*f***, respectively. In the former case, one can extract the phase accumulation of the electron wave packets under the influence of the strong IR field, which reached an intensity of approximately 10^{13} W cm^{-2} in the experimental region. In the latter case, the recorded image reveals the opposite momentum shifts acquired by consecutive electron wave packets and an interference pattern that is particularly apparent perpendicular to the polarization axis. A detailed analysis and comparison with theoretical calculations (solving the time-dependent Schrödinger equation) revealed the interference patterns to be consistent with the fact that for an Ar ground-state *p*-orbital, the $m = 0$ component (signifying the alignment of the orbital along the polarization axis) changes sign across a plane perpendicular to the polarization axis, whereas the $m = \pm 1$ components are symmetric with respect to this plane. The images recorded so far do not allow the recovery of the full momentum wave function. However, one may well imagine that analysis of the full momentum space projection and acquisition of these projections using different values (and polarization directions) of $A(\tau)$ would allow full retrieval. In the future, attempts will be made to perform the experiment using the idealized case of a train of two attosecond pulses.

5.3. Further Experiments with Attosecond Pulse Trains

Recently Johnsson et al. (104) used trains of attosecond pulses generated in Xe atoms to investigate He ionization in the presence of an IR laser field. This introduces an important new element into the electron dynamics compared to the wave-packet interferometry measurements presented in Reference 102. The attosecond pulses now have a central frequency below the ionization energy of He and therefore can excite bound states that are subsequently ionized by the IR field (104). The two-color ionization yield depends in an oscillatory manner on the delay of the attosecond pulse train with respect to the electric field oscillations of the IR field. Remarkably, a detailed simulation of the experimental results revealed that this behavior would not

be expected if the experiment is performed with an isolated attosecond pulse, but is a direct consequence of the fact that the excitation occurs by a train of pulses.

In experiments similar to the above-mentioned He experiments, Mauritsson et al. (105) have used low-energy photoelectrons injected by attosecond pulses generated in Ar. These recollide with the He^+ ion as a result of its interaction with the IR field, and the final electron momentum distributions provide a tool for probing the non-Coulombic part of the atomic potential.

6. TOWARD ATTOSECOND APPLICATIONS IN CHEMISTRY

Molecular experiments involving high-harmonic radiation have thus far been sparse. Using harmonics as a pump pulse, Zamith et al. (106) photodissociated the acetylene molecule, generating 133-nm radiation as the third harmonic of the second harmonic of a Ti:sapphire laser and using time-resolved photoelectron spectroscopy to monitor the dynamics on femtosecond timescales. Using the XUV laser pulses as a probe, Nugent-Glandorf and coworkers (107) monitored the 400-nm dissociation of Br_2 on femtosecond timescales (again using time-resolved photoelectron spectroscopy), whereas recently Lépine et al. (108) used dissociative ionization by a comb of harmonics and angle- and energy-resolved detection of fragment ions using a velocity-map imaging spectrometer to monitor time-dependent strong-field alignment in N_2, O_2, and CO_2. No experiment has been performed in which an isolated attosecond pulse or an attosecond pulse train initiates or extracts an attosecond response from a molecule.

The use of attosecond pulses in molecular dynamics studies should be of considerable interest. When molecular dynamics are induced in a laser pump-probe experiment, electronic excitation generally precedes nuclear motion. One can then use attosecond pulses to monitor both the electronic rearrangement during such a photochemical event and the initial stages of the nuclear motion. In doing so, the short wavelengths of the attosecond laser pulses allow both absorption and diffraction to be used to extract information. When photon energies of several tens of electron volts are employed, the attosecond pulses interact primarily with valence electrons. However, when the photon energies of the attosecond pulses are increased beyond 100 eV, inner-shell excitation becomes possible, and one enters the regime in which X-ray absorption near-edge structure (within ~10 eV of an absorption edge), near-edge X-ray absorption fine structure (between 10 and 50 eV from an absorption edge), and extended X-ray absorption fine structure (between 50 and 1000 eV above an absorption edge) become observable (109). These techniques have been used primarily without time resolution at synchrotron facilities, providing insight into the chemical and structural environment surrounding the atom from which the core electron is removed. With XUV pulses produced using HHG, it may become possible to obtain this information on femtosecond, or even attosecond, timescales.

In the examples discussed above, the role of the attosecond pulse is to probe ultrafast electronic and nuclear dynamics. When attosecond pulses are used to initiate electron dynamics in molecules, the high photon energy of the attosecond pulse generally results in ionization. Remacle & Levine (110) and Cederbaum and coworkers (111, 112) considered recently the formation of electronic wave packets as a result

of the removal of an electron on attosecond timescales. Because the electron-hole density that results from removing one of the electrons from the highest-occupied molecular orbital (HOMO) of a neutral molecule (doubly occupied) generally differs from the electron-hole density in the singly occupied HOMO of the cation formed on ionization, ultrafast removal of an electron not only forms the ground electronic state of the cation, but also forms a coherent superposition of electronic states. Comparing a wide range of electronic systems, Breidbach & Cederbaum (112) observed that the sudden removal of an electron is accompanied by a characteristic time response completed in approximately 50 as. This time response is interpreted in terms of a filling—on ionization—of the exchange-correlation hole associated with the ionized electron by its neighboring electrons. Remacle & Levine (110) have argued that the sudden ionization of a molecule may lead to electron transport across the ionic structure that is formed. For example, the photoionization of the neutral tetrapeptide molecule $TrpLeu_3$ is expected to lead to the population of the HOMO-1 and the HOMO of the $TrpLeu_3^+$ cation. The shape of these orbitals and the 3-eV energy splitting between the two orbitals suggest that electron transfer from one end of the molecule to the other occurs in less than 1 fs.

6.1. Carrier-Envelope-Phase Control of Electron Localization in Molecular Dissociation

Although photoinduced electron transfer in molecules has not been observed on attosecond timescales, we have illustrated recently a crucial role of ultrafast driven intramolecular electronic motion when molecules are exposed to intense laser fields. We investigated experimentally the extent to which few-cycle CEP-locked laser radiation could be used to localize an electron inside a molecule by performing an experiment where the dissociation of D_2^+ into $D^+ + D$ was monitored (58). Measurements of the angle-resolved kinetic energy distributions of the D^+ fragments (related by momentum conservation to the ejection of the D atom that contains the electron in the system) showed (see **Figure 5*a***) that the direction of the electron emission could be controlled and localized using the CEP of the 5-fs near-IR laser. The mechanism that allows this control consists of three elements (**Figure 5*b***). The first step is the ionization of the neutral D_2 molecule, leading to the formation of the D_2^+ ion in its $2s\sigma_g^+$ ground state. A measurement of the polarization dependence of the fragmentation process shows that fragments are produced only in the kinetic energy range where the asymmetry occurs (3–8 eV) when the polarization of the laser is linear. Because the main consequence of changing the laser's polarization is its influence on the probability that this electron can undergo a recollision with the D_2^+ molecular ion, this strongly suggests that—as a second step—a recollision of the electron pulled out of the molecule when the D_2^+ ion is formed initiates the dissociation of the molecular ion by promoting it to the repulsive $2p\sigma_u^+$ state (113).

The observation of an asymmetry, however, requires breaking the parity of the electronic state. This is accomplished through the continued action of the laser on the second, remaining electron. As the molecule dissociates, population is stimulated

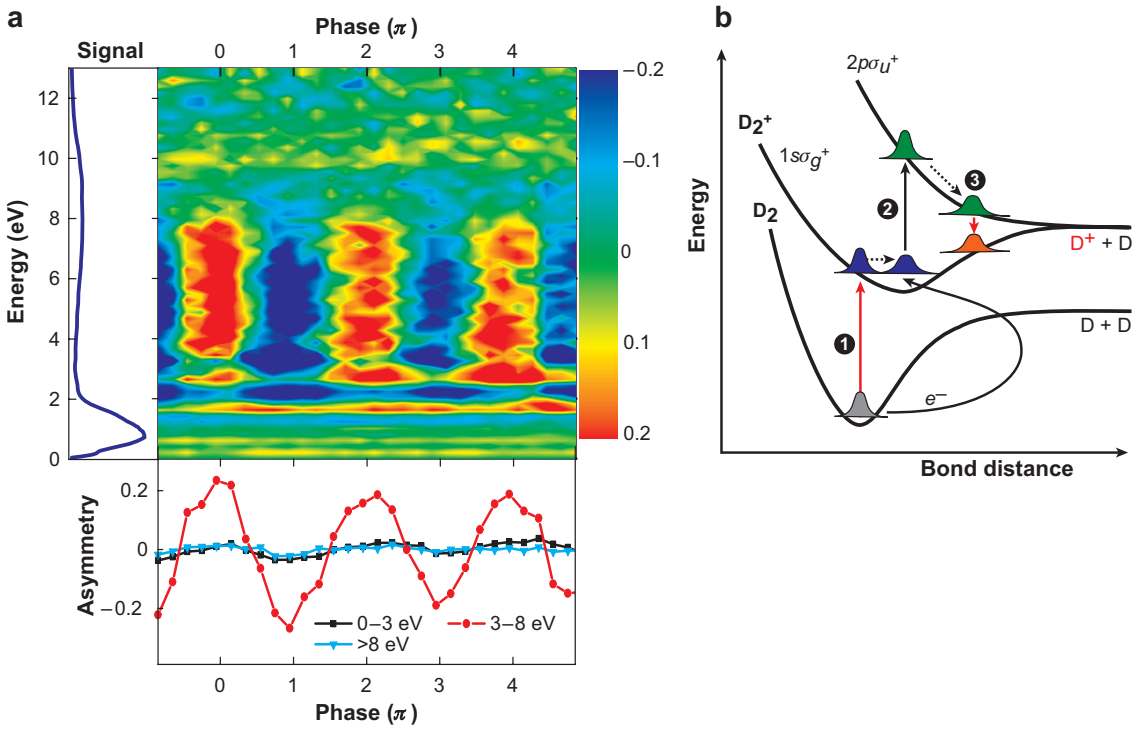

Figure 5

(*a*) Experimental results illustrating that, in the dissociative ionization of D_2 into $D^+ + D$ for fragments with a kinetic energy between 3 and 8 eV, one can control the direction of the D^+ ion emission, and thus the localization of the electron, using the carrier envelope phase (CEP) of a few-cycle laser (*center panel*). The kinetic energy distribution of the D^+ fragments is shown on the left panel, and the bottom panel shows an integration of the asymmetry for different energy ranges. (*b*) Mechanism for the control of electron localization in D_2^+ using a few-cycle CEP-stable laser pulse. Upon the formation of the D_2^+ ion (*step 1*), a recollision promotes the molecule to a repulsive curve (*step 2*), initiating the dissociation. In the course of the dissociation, stimulated emission drives part of the population back toward the ground state (*step 3*), breaking the parity of the electronic wave function.

down from the $2p\sigma_u^+$ state to the $1s\sigma_g^+$ state, leading to a situation where the molecule is in a coherent superposition state (step three) and the electron oscillates between the two ions with a period initially governed by the laser (96, 114). As the energy gap between the $2p\sigma_u^+$ state and the $1s\sigma_g^+$ state becomes less than the photon energy of the laser, the coupling between the two electronic states weakens, and the electron becomes trapped on either of the two D^+ ions, incapable of passing over the barrier that has built up between the two. The essence of the observed control, therefore, as further supported recently by more detailed theoretical treatments (115, 116), is an attosecond-timescale electronic motion. This experiment demonstrates that (*a*) attosecond electron motion is relevant to chemical processes and (*b*) attosecond shaping of the light field in a femtosecond pulse can be used to control it. The results

are the first example of the direct light-field control of intramolecular electronic motion and may provide an initial clue for the control of intramolecular electron transfer processes using waveform-controlled light fields in more complex systems.

7. OUTLOOK

This article reviews the recent emergence of attosecond science. Using the technique of HHG, it has now become possible to generate isolated attosecond laser pulses and/or trains of attosecond laser pulses in a number of laser laboratories worldwide. Attosecond science has captured the imagination of many researchers, leading to exponential growth in the number of publications devoted to the topic, as well as widespread anticipation regarding its future impact. Building on some of the early experiments discussed above, we may expect to see further applications of attosecond pulses toward the elucidation of ultrafast electron dynamics in atoms, as well as initial attempts to observe, and possibly control, electronic motion on attosecond timescales in molecules. Furthermore, we will witness the application of attosecond laser pulses toward areas of science where studies on multielectron dynamics have only recently started, such as investigations into the electronic response accompanying collective electron dynamics (plasmons) in nanomaterials. For example, Stockman et al. (117) proposed recently a technique called attosecond nanoplasmonic field microscope for studies of collective electron dynamics in surface nanosystems with combined attosecond temporal and nanometer spatial resolution. The approach is based on attosecond streaking and photoelectron emission microscopy and, similar to streaking experiments in the gas phase, utilizes attosecond XUV pulses synchronized to a few-cycle optical laser field. The optical field is used to excite collective electron motions, and a temporally delayed XUV pulse that leads to the emission of electrons from the plasmonic nanosystem probes the dynamics. For suitable conditions, the energy of these photoelectrons depends on the instantaneous potential of the plasmonic field at the time of their emission (117). Spatially resolved detection of the photoelectrons in a photoelectron emission microscope enables the direct observation of the nanometer-localized attosecond dynamics of plasmonic fields. The integration of attosecond science and nanotechnology will yield unprecedented insight into collective, multielectron behavior, in which the information contained in a time-resolved experiment may significantly exceed the information that can be obtained by other (non-time-resolved) means.

To maintain the current growth rate of attosecond science, and to accomplish the goals outlined above, further development of technical capabilities is absolutely vital. In doing so, attention not only needs to go toward developing attosecond sources, but also to the complete design of the attosecond experiment, including developing specialized optics (118–120) and detectors (121). With regards to detection, we anticipate that the interpretation of attosecond experiments will increasingly require the correlated detection of as many reaction products as possible, using techniques such as (cold-target) recoil-ion momentum spectroscopy (122). The application of attosecond studies toward molecules will require that attosecond XUV pulses, and so far nonexistent few- or single-cycle UV pulses, can be generated with sufficient

intensity to allow UV-XUV or XUV-XUV pump-probe experiments. Several recently started developments have significant potential for overcoming these current limitations, such as the generation of attosecond pulses using surface harmonic generation (48), interferometric polarization gating (using many-cycle terawatt-level driver lasers) (51), and relativistic generation in the λ^3-regime (123). In the next few years, these methods may allow the production of isolated attosecond pulses that are as intense as the pulses presently generated as part of an attosecond pulse train. A new source, in which the intensity of the XUV light is no longer an issue, has recently emerged: At XUV free electron lasers, such as the FLASH laser in Hamburg (124), focused XUV intensities in excess of 10^{15} W cm^{-2} are available presently, suggesting that we may soon witness the first XUV-XUV pump-probe experiments there, albeit with femtosecond time resolution. However, many ideas exist for shortening the pulse duration of free electron lasers, extending all the way into the attosecond regime (125).

For the applications of attosecond science in physical chemistry and elsewhere to reach their full potential, a significant challenge also exists with regard to the development of theoretical tools. If we are to use attosecond pulses to gain a better understanding of electron correlation, the further development of computational tools such as multiconfiguration time-dependent Hartree-Fock methods (126, 127) or calculations using time-dependent adiabatic states (128) is absolutely vital. Similarly, the utility of time-dependent density-functional methods should be critically assessed (129).

SUMMARY POINTS

1. Using HHG, isolated attosecond pulses and attosecond pulse trains can be reproducibly and reliably generated.
2. Using techniques such as the attosecond streak camera and RABBITT, one can characterize fully the temporal structure of isolated attosecond pulses and attosecond pulse trains. Pulse durations down to 130 as have already been demonstrated.
3. Researchers have used isolated attosecond pulses to measure the lifetimes for Auger decay in atoms, as well as the subcycle time dependence of strong-field ionization processes.
4. Using trains of attosecond pulses, investigators have developed a new type of electron wave-packet interferometry that allows the retrieval of the amplitude and phase of an electronic wave function.
5. As recently shown in a demonstration on the dissociative ionization of D_2, CEP-phase locked laser pulses can be used to control the localization of electrons in molecules, paving the way for observing and controlling attosecond-timescale electron dynamics in molecules.

FUTURE ISSUES

1. To be able to perform attosecond XUV pump–attosecond XUV probe experiments, we need to increase the intensity of available attosecond light sources, using one or more of the approaches discussed above (surface harmonic generation, interferometric polarization gating, relativistic harmonic generation, attosecond pulse generation at XUV free electron lasers).
2. Attosecond source development toward not only higher brightness but also higher energies and shorter pulse durations and the characterization of these pulses need to be supplemented by extensive work on XUV optics that will allow tailoring of the spectrum and the chirp of the attosecond laser pulses.
3. The development of few-femtosecond VUV-UV sources will extend current possibilities to study attosecond electron dynamics in molecular systems.
4. Experimental developments need to be accompanied by significant development of theoretical tools for the computation and understanding of multielectron dynamics.
5. Attosecond studies on electron correlation and collective electron motion in complex systems are of great interest and will be pursued increasingly.

DISCLOSURE STATEMENT

The authors are not aware of any biases that might be perceived as affecting the objectivity of this review.

ACKNOWLEDGMENT

This work is part of the research program of the Stichting voor Fundamenteel Onderzoek der Materie (FOM), which is financially supported by the Nederlandse organisatie voor Wetenschappelijk Onderzoek (NWO). Financial support from the Marie Curie Research Training Network XTRA is gratefully acknowledged. M.F. Kling acknowledges support from IEF and ERG grants of the European Community and from the Emmy-Noether program of the DFG.

LITERATURE CITED

1. Föhlisch A, Feulner P, Hennies F, Fink A, Menzel D, et al. 2005. Direct observation of electron dynamics in the attosecond domain. *Nature* 436:373–76
2. Zewail AH. 2000. Femtochemistry: atomic-scale dynamics of the chemical bond using ultrafast lasers (Nobel lecture). *Angew. Chem. Int. Ed. Engl.* 39:2587–631
3. Gallagher TF. 1988. Rydberg atoms. *Rep. Prog. Phys.* 51:143–88
4. ten Wolde A, Noordam LD, Lagendijk A, Vandenheuvell HBV. 1988. Observation of radially localized atomic electron wave packets. *Phys. Rev. Lett.* 61:2099–101

5. Vrakking MJJ, Lee YT. 1995. Lifetimes of Rydberg states in zero-electron-kinetic-energy experiments. 1. Electric-field-induced and collisional enhancement of NO predissociation lifetimes. *J. Chem. Phys.* 102:8818–32
6. Vrakking MJJ, Lee YT. 1995. Lifetimes of Rydberg states in zero-electron-kinetic-energy experiments. 2. Electric-field-induced and collisional enhancement of Xe autoionization lifetimes. *J. Chem. Phys.* 102:8833–41
7. Schenkel B, Biegert J, Keller U, Vozzi C, Nisoli M, et al. 2003. Generation of 3.8-fs pulses from adaptive compression of a cascaded hollow fiber supercontinuum. *Opt. Lett.* 28:1987–89
8. Nisoli M, DeSilvestri S, Svelto O, Szipocs R, Ferencz K, et al. 1997. Compression of high-energy laser pulses below 5 fs. *Opt. Lett.* 22:522–24
9. Hänsch TW. 1990. A proposed sub-femtosecond pulse synthesizer using separate phase-locked laser oscillators. *Opt. Commun.* 80:71–75
10. Farkas G, Toth C. 1992. Proposal for attosecond light-pulse generation using laser-induced multiple-harmonic conversion processes in rare gases. *Phys. Lett. A* 168:447–50
11. Antoine P, L'Huillier A, Lewenstein M. 1996. Attosecond pulse trains using high-order harmonics. *Phys. Rev. Lett.* 77:1234–37
12. Antoine P, Milosevic DB, L'Huillier A, Gaarde MB, Salieres P, Lewenstein M. 1997. Generation of attosecond pulses in macroscopic media. *Phys. Rev. A* 56:4960–69
13. Harris SE, Sokolov AV. 1998. Subfemtosecond pulse generation by molecular modulation. *Phys. Rev. Lett.* 81:2894–97
14. Seres J, Seres E, Verhoef AJ, Tempea G, Strelill C, et al. 2005. Source of coherent kiloelectronvolt X-rays. *Nature* 433:596
15. **Paul PM, Toma ES, Breger P, Mullot G, Auge F, et al. 2001. Observation of a train of attosecond pulses from high harmonic generation. *Science* 292:1689–92**
16. **Hentschel M, Kienberger R, Spielmann C, Reider GA, Milosevic N, et al. 2001. Attosecond metrology. *Nature* 414:509–13**
17. Brabec T, Krausz F. 2000. Intense few-cycle laser fields: frontiers of nonlinear optics. *Rev. Mod. Phys.* 72:545–91
18. Agostini P, DiMauro LF. 2004. The physics of attosecond light pulses. *Rep. Prog. Phys.* 67:813–55
19. Scrinzi A, Ivanov MY, Kienberger R, Villeneuve DM. 2006. Attosecond physics. *J. Phys. B At. Mol. Opt. Phys.* 39:R1–37
20. Corkum PB, Krausz F. 2007. Attosecond science. *Nat. Phys.* 3:381–87
21. Pfeifer T, Spielmann C, Gerber G. 2006. Femtosecond X-ray science. *Rep. Prog. Phys.* 69:443–505
22. Corkum PB, Ivanov MY, Wright JS. 1997. Subfemtosecond processes in strong laser fields. *Annu. Rev. Phys. Chem.* 48:387–406
23. **Corkum PB. 1993. Plasma perspective on strong-field multiphoton ionization. *Phys. Rev. Lett.* 71:1994–97**
24. Lewenstein M, Balcou P, Ivanov MY, L'Huillier A, Corkum PB. 1994. Theory of high-harmonic generation by low-frequency laser fields. *Phys. Rev. A* 49:2117–32

15. First report of the generation of a train of attosecond pulses and introduction of the RABBITT technique for the characterization of these trains.

16. First report of the generation of an isolated attosecond pulse and introduction of the attosecond streak camera as a means to measure the duration of these pulses.

23. Introduces the semiclassical picture that underlies HHG and its ability to produce attosecond laser pulses.

25. Aseyev SA, Ni Y, Frasinski LJ, Muller HG, Vrakking MJJ. 2003. Attosecond angle-resolved photoelectron spectroscopy. *Phys. Rev. Lett.* 91:223902
26. Mairesse Y, de Bohan A, Frasinski LJ, Merdji H, Dinu LC, et al. 2003. Attosecond synchronization of high-harmonic soft X-rays. *Science* 302:1540–43
27. Ferray M, L'Huillier A, Li XF, Lompre LA, Mainfray G, Manus C. 1988. Multiple-harmonic conversion of 1064-nm radiation in rare gases. *J. Phys. B At. Mol. Opt. Phys.* 21:L31–35
28. Kienberger R, Hentschel M, Uiberacker M, Spielmann C, Kitzler M, et al. 2002. Steering attosecond electron wave packets with light. *Science* 297:1144–48
29. Baltuska A, Udem T, Uiberacker M, Hentschel M, Goulielmakis E, et al. 2003. Attosecond control of electronic processes by intense light fields. *Nature* 421:611–15
30. Kienberger R, Goulielmakis E, Uiberacker M, Baltuska A, Yakovlev V, et al. 2004. Atomic transient recorder. *Nature* 427:817–21
31. Cavalieri AL, Goulielmakis E, Horvath B, Helml W, Schultze M, et al. 2007. Intense 1.5-cycle near infrared laser waveforms and their use for the generation of ultra-broadband soft-X-ray harmonic continua. *New J. Phys.* 9:242
32. Christov IP, Murnane MM, Kapteyn HC. 1997. High-harmonic generation of attosecond pulses in the "single-cycle" regime. *Phys. Rev. Lett.* 78:1251–54
33. Udem T, Holzwarth R, Hänsch TW. 2002. Optical frequency metrology. *Nature* 416:233–37
34. Fortier TM, Ashby N, Bergquist JC, Delaney MJ, Diddams SA, et al. 2007. Precision atomic spectroscopy for improved limits on variation of the fine structure constant and local position invariance. *Phys. Rev. Lett.* 98:070801
35. Hänsch TW. 2006. Nobel lecture: passion for precision. *Rev. Mod. Phys.* 78:1297–309
36. Hall JL. 2006. Nobel lecture: defining and measuring optical frequencies. *Rev. Mod. Phys.* 78:1279–95
37. Paulus GG, Lindner F, Walther H, Baltuska A, Goulielmakis E, et al. 2003. Measurement of the phase of few-cycle laser pulses. *Phys. Rev. Lett.* 91:253004
38. Apolonski A, Dombi P, Paulus GG, Kakehata M, Holzwarth R, et al. 2004. Observation of light-phase-sensitive photoemission from a metal. *Phys. Rev. Lett.* 92:073902
39. Kress M, Loffler T, Thomson MD, Dorner R, Gimpel H, et al. 2006. Determination of the carrier-envelope phase of few-cycle laser pulses with terahertz-emission spectroscopy. *Nat. Phys.* 2:327–31
40. Kling MF, Rauschenberger J, Verhoef AJ, Hasovic E, Uphues T, et al. 2007. Imaging of carrier-envelope phase effects in above-threshold ionization with intense few-cycle laser fields. *New J. Phys.* Submitted
41. Haworth CA, Chipperfield LE, Robinson JS, Knight PL, Marangos JP, Tisch JWG. 2007. Half-cycle cutoffs in harmonic spectra and robust carrier-envelope phase retrieval. *Nat. Phys.* 3:52–57
42. Hergott JF, Kovacev M, Merdji H, Hubert C, Mairesse Y, et al. 2002. Extreme-UV high-order harmonic pulses in the microjoule range. *Phys. Rev. A* 66:021801
43. Corkum PB, Burnett NH, Ivanov MY. 1994. Subfemtosecond pulses. *Opt. Lett.* 19:1870–72

44. Kovacev M, Mairesse Y, Priori E, Merdji H, Tcherbakoff O, et al. 2003. Temporal confinement of the harmonic emission through polarization gating. *Eur. Phys. J. D* 26:79–82
45. Lopez-Martens R, Mauritsson J, Johnsson P, L'Huillier A, Tcherbakoff O, et al. 2004. Time-resolved ellipticity gating of high-order harmonic emission. *Phys. Rev. A* 69:053811
46. Sola IJ, Mevel E, Elouga L, Constant E, Strelkov V, et al. 2006. Controlling attosecond electron dynamics by phase-stabilized polarization gating. *Nat. Phys.* 2:319–22
47. Sansone G, Benedetti E, Calegari F, Vozzi C, Avaldi L, et al. 2006. Isolated single-cycle attosecond pulses. *Science* 314:443–46
48. Tsakiris GD, Eidmann K, Meyer-ter-Vehn J, Krausz F. 2006. Route to intense single attosecond pulses. *New J. Phys.* 8:19
49. Queré F, Thaury C, Monot P, Dobosz S, Martin P, et al. 2006. Coherent wake emission of high-order harmonics from overdense plasmas. *Phys. Rev. Lett.* 96:125004
50. Dromey B, Zepf M, Gopal A, Lancaster K, Wei MS, et al. 2006. High harmonic generation in the relativistic limit. *Nat. Phys.* 2:456–59
51. Tzallas P, Skantzakis E, Kalpouzos C, Benis EP, Tsakiris GD, Charalambidis D. 2007. Generation of intense continuum extreme-ultraviolet radiation by many-cycle laser fields. *Nat. Phys.* 3:846–50
52. Zamith S, Ni Y, Gurtler A, Noordam LD, Muller HG, Vrakking MJJ. 2004. Control of atomic ionization by two-color few-cycle pulses. *Opt. Lett.* 29:2303–5
53. Siedschlag C, Muller HG, Vrakking MJJ. 2005. Generation of isolated attosecond pulses by two-color laser fields. *Laser Phys.* 15:916–25
54. Pfeifer T, Gallmann L, Abel MJ, Neumark DM, Leone SR. 2006. Single attosecond pulse generation in the multicycle-driver regime by adding a weak second harmonic. *Opt. Lett.* 31:975–77
55. Pfeifer T, Gallmann L, Abel MJ, Nagel PM, Neumark DM, Leone SR. 2006. Heterodyne mixing of laser fields for temporal gating of high-order harmonic generation. *Phys. Rev. Lett.* 97:163901
56. Mauritsson J, Johnsson P, Gustafsson E, L'Huillier A, Schafer KJ, Gaarde MB. 2006. Attosecond pulse trains generated using two color laser fields. *Phys. Rev. Lett.* 97:013001
57. Paulus GG, Grasbon F, Walther H, Villoresi P, Nisoli M, et al. 2001. Absolute-phase phenomena in photoionization with few-cycle laser pulses. *Nature* 414:182–84
58. Kling MF, Siedschlag C, Verhoef AJ, Khan JI, Schultze M, et al. 2006. Control of electron localization in molecular dissociation. *Science* 312:246–48
59. Niikura H, Corkum PB. 2007. Attosecond and Angstrom science. *Adv. At. Mol. Opt. Phys.* 54:511–48
60. Itatani J, Levesque J, Zeidler D, Niikura H, Pepin H, et al. 2004. Tomographic imaging of molecular orbitals. *Nature* 432:867–71
61. Rosca-Pruna F, Vrakking MJJ. 2001. Experimental observation of revival structures in picosecond laser-induced alignment of I_2. *Phys. Rev. Lett.* 87:153902

58. First experiment controlling electron localization in a molecule on attosecond timescales, using the reproducible waveform of a CEP-stabilized laser.

60. First experimental demonstration that in HHG interference between the recollision electron and the ground-state wave function encodes information into the high-harmonic spectrum.

62. Lein M, Hay N, Velotta R, Marangos JP, Knight PL. 2002. Role of the intramolecular phase in high-harmonic generation. *Phys. Rev. Lett.* 88:183903
63. Kanai T, Minemoto S, Sakai H. 2005. Quantum interference during high-order harmonic generation from aligned molecules. *Nature* 435:470–74
64. Zuo T, Bandrauk AD, Corkum PB. 1996. Laser-induced electron diffraction: a new tool for probing ultrafast molecular dynamics. *Chem. Phys. Lett.* 259:313–20
65. Spanner M, Smirnova O, Corkum PB, Ivanov MY. 2004. Reading diffraction images in strong field ionization of diatomic molecules. *J. Phys. B At. Mol. Opt. Phys.* 37:L243–50
66. Niikura H, Legare F, Hasbani R, Bandrauk AD, Ivanov MY, et al. 2002. Sub-laser-cycle electron pulses for probing molecular dynamics. *Nature* 417:917–22
67. Niikura H, Legare F, Hasbani R, Ivanov MY, Villeneuve DM, Corkum PB. 2003. Probing molecular dynamics with attosecond resolution using correlated wave packet pairs. *Nature* 421:826–29
68. Baker S, Robinson JS, Haworth CA, Teng H, Smith RA, et al. 2006. Probing proton dynamics in molecules on an attosecond time scale. *Science* 312:424–27
69. Wagner NL, Wuest A, Christov IP, Popmintchev T, Zhou XB, et al. 2006. Monitoring molecular dynamics using coherent electrons from high harmonic generation. *Proc. Natl. Acad. Sci. USA* 103:13279–85
70. Mairesse Y, Queré F. 2005. Frequency-resolved optical gating for complete reconstruction of attosecond bursts. *Phys. Rev. A* 71:011401
71. Dinu LC, Muller HG, Kazamias S, Mullot G, Auge F, et al. 2003. Measurement of the subcycle timing of attosecond XUV bursts in high-harmonic generation. *Phys. Rev. Lett.* 91:063901
72. Mairesse Y, de Bohan A, Frasinski LJ, Merdji H, Dinu LC, et al. 2004. Optimization of attosecond pulse generation. *Phys. Rev. Lett.* 93:163901
73. Itatani J, Queré F, Yudin GL, Ivanov MY, Krausz F, Corkum PB. 2002. Attosecond streak camera. *Phys. Rev. Lett.* 88:173903
74. Kitzler M, Milosevic N, Scrinzi A, Krausz F, Brabec T. 2002. Quantum theory of attosecond XUV pulse measurement by laser dressed photoionization. *Phys. Rev. Lett.* 88:173904
75. Schultze M, Goulielmakis E, Uiberacker M, Hofstetter M, Kim J, et al. 2007. Powerful 170-attosecond XUV pulses generated with few-cycle laser pulses and broadband multilayer optics. *New J. Phys.* 9:243
76. Goulielmakis E, Yakovlev VS, Cavalieri AL, Uiberacker M, Pervak V, et al. 2007. Attosecond control and measurement: lightwave electronics. *Science* 317:769–75
77. Drescher M, Hentschel M, Kienberger R, Uiberacker M, Yakovlev V, et al. 2002. Time-resolved atomic inner-shell spectroscopy. *Nature* 419:803–7
78. Goulielmakis E, Uiberacker M, Kienberger R, Baltuska A, Yakovlev V, et al. 2004. Direct measurement of light waves. *Science* 305:1267–69
79. Eppink ATJB, Parker DH. 1997. Velocity map imaging of ions and electrons using electrostatic lenses: application in photoelectron and photofragment ion imaging of molecular oxygen. *Rev. Sci. Instrum.* 68:3477–84
80. Uphues T, Zherebtsov S, Goulielmakis E, Schultze M, Uiberacker M, et al. 2007. 3D attosecond streak camera. In preparation

77. First experiment using isolated attosecond laser pulses to time resolve an atomic process, namely the ejection of an Auger electron from Kr atoms following their ionization by a 90-eV attosecond pulse.

81. Tzallas P, Charalambidis D, Papadogiannis NA, Witte K, Tsakiris GD. 2003. Direct observation of attosecond light bunching. *Nature* 426:267–71
82. Nikolopoulos LAA, Benis EP, Tzallas P, Charalambidis D, Witte K, Tsakiris GD. 2005. Second order autocorrelation of an XUV attosecond pulse train. *Phys. Rev. Lett.* 94:113905
83. Sekikawa T, Kosuge A, Kanai T, Watanabe S. 2004. Nonlinear optics in the extreme UV. *Nature* 432:605–8
84. Sekikawa T, Kanai T, Watanabe S. 2003. Frequency-resolved optical gating of femtosecond pulses in the extreme UV. *Phys. Rev. Lett.* 91:103902
85. Kosuge A, Sekikawa T, Zhou X, Kanai T, Adachi S, Watanabe S. 2006. Frequency-resolved optical gating of isolated attosecond pulses in the extreme UV. *Phys. Rev. Lett.* 97:263901
86. Nabekawa Y, Shimizu T, Okino T, Furusawa K, Hasegawa H, et al. 2006. Conclusive evidence of an attosecond pulse train observed with the mode-resolved autocorrelation technique. *Phys. Rev. Lett.* 96:083901
87. Nabekawa Y, Shimizu T, Okino T, Furusawa K, Hasegawa H, et al. 2006. Interferometric autocorrelation of an attosecond pulse train in the single-cycle regime. *Phys. Rev. Lett.* 97:153904
88. Varju K, Mairesse Y, Agostini P, Breger P, Carre B, et al. 2005. Reconstruction of attosecond pulse trains using an adiabatic phase expansion. *Phys. Rev. Lett.* 95:243901
89. Varju K, Mairesse Y, Carre B, Gaarde MB, Johnsson P, et al. 2005. Frequency chirp of harmonic and attosecond pulses. *J. Mod. Opt.* 52:379–94
90. Iaconis C, Walmsley IA. 1998. Spectral phase interferometry for direct electric-field reconstruction of ultrashort optical pulses. *Opt. Lett.* 23:792–94
91. Queré F, Itatani J, Yudin GL, Corkum PB. 2003. Attosecond spectral shearing interferometry. *Phys. Rev. Lett.* 90:073902
92. Cormier E, Corner L, Kosik EM, Walmsley IA, Wyatt AS. 2005. Spectral phase interferometry for complete reconstruction of attosecond pulses. *Laser Phys.* 15:909–15
93. Mairesse Y, Gobert O, Breger P, Merdji H, Meynadier P, et al. 2005. High harmonic XUV spectral phase interferometry for direct electric-field reconstruction. *Phys. Rev. Lett.* 94:173903
94. Dudovich N, Smirnova O, Levesque J, Mairesse Y, Ivanov MY, et al. 2006. Measuring and controlling the birth of attosecond XUV pulses. *Nat. Phys.* 2:781–86
95. Hu SX, Collins LA. 2006. Attosecond pump probe: exploring ultrafast electron motion inside an atom. *Phys. Rev. Lett.* 96:073004
96. Yudin GL, Chelkowski S, Itatani J, Bandrauk AD, Corkum PB. 2005. Attosecond photoionization of coherently coupled electronic states. *Phys. Rev. A* 72:051401
97. Uiberacker M, Uphues T, Schultze M, Verhoef AJ, Yakovlev V, et al. 2007. Attosecond real-time observation of electron tunnelling in atoms. *Nature* 446:627–32
98. Becker W, Grasbon F, Kopold R, Milosevic DB, Paulus GG, Walther H. 2002. Above-threshold ionization: from classical features to quantum effects. *Adv. At. Mol. Opt. Phys.* 48:35–98

97. First experiment using isolated attosecond laser pulses to extract information on bound-state electron dynamics on attosecond timescales and using the subcycle time dependence of strong-field ionization in attosecond pump-probe experiments.

99. Yudin GL, Ivanov MY. 2001. Nonadiabatic tunnel ionization: looking inside a laser cycle. *Phys. Rev. A* 64:013409
100. Vrakking MJJ, Yakovlev V, Kling MF, Muller HG, Ivanov M, Krausz F. 2007. Sub-cycle time-dependence of strong field ionization. In preparation
101. Johnsson P, Lopez-Martens R, Kazamias S, Mauritsson J, Valentin C, et al. 2005. Attosecond electron wave packet dynamics in strong laser fields. *Phys. Rev. Lett.* 95:013001
102. Remetter T, Johnsson P, Mauritsson J, Varju K, Ni Y, et al. 2006. Attosecond electron wave packet interferometry. *Nat. Phys.* 2:323–26
103. Varju K, Johnsson P, Mauritsson J, Remetter T, Ruchon T, et al. 2006. Angularly resolved electron wave packet interferences. *J. Phys. B At. Mol. Opt. Phys.* 39:3983–91
104. Johnsson P, Mauritsson J, Remetter T, L'Huillier A, Schafer KJ. 2007. Attosecond control of ionization by wave packet interferences. Submitted
105. Mauritsson J, Johnsson P, Gustafsson E, Swoboda M, Ruchon T, et al. 2007. Coherent electron scattering captured by an attosecond quantum stroboscope. Submitted
106. Zamith S, Blanchet V, Girard B, Andersson J, Sorensen SL, et al. 2003. The predissociation of highly excited states in acetylene by time-resolved photoelectron spectroscopy. *J. Chem. Phys.* 119:3763–73
107. Nugent-Glandorf L, Scheer M, Samuels DA, Mulhisen AM, Grant ER, et al. 2001. Ultrafast time-resolved soft X-ray photoelectron spectroscopy of dissociating Br_2. *Phys. Rev. Lett.* 8719:193002
108. Lépine F, Kling M, Ni Y, Khan J, Ghafur O, et al. 2007. Short XUV pulses to characterize field-free molecular alignment. *J. Mod. Opt.* 54:953–66
109. Koningsberger DC, Prins R, eds. 1988. *X-Ray Absorption*. New York: Wiley
110. Remacle F, Levine RD. 2006. An electronic time scale in chemistry. *Proc. Nat. Acad. Sci. USA* 103:6793–98
111. Hennig H, Breidbach J, Cederbaum LS. 2005. Electron correlation as the driving force for charge transfer: charge migration following ionization in *N*-methyl acetamide. *J. Phys. Chem. A* 109:409–14
112. Breidbach J, Cederbaum LS. 2005. Universal attosecond response to the removal of an electron. *Phys. Rev. Lett.* 94:033901
113. Legare F, Litvinyuk IV, Dooley PW, Queré F, Bandrauk AD, et al. 2003. Time-resolved double ionization with few cycle laser pulses. *Phys. Rev. Lett.* 91:093002
114. Bandrauk AD, Chelkowski S, Nguyen HS. 2004. Attosecond localization of electrons in molecules. *Int. J. Q. Chem.* 100:834–44
115. Graefe S, Ivanov M. 2007. Effective fields in laser-driven electron recollision and charge localization. *Phys. Rev. Lett.* 99:163603
116. Tong XM, Lin CD. 2007. Dynamics of light-field control of molecular dissociation at the few-cycle limit. *Phys. Rev. Lett.* 98:123002
117. Stockman MI, Kling MF, Kleineberg U, Krausz F. 2007. Attosecond nanoplasmonic field microscope. *Nat. Photonics* 1:539–44
118. Lopez-Martens R, Varju K, Johnsson P, Mauritsson J, Mairesse Y, et al. 2005. Amplitude and phase control of attosecond light pulses. *Phys. Rev. Lett.* 94:033001

102. First use of attosecond pulse trains to obtain information about atomic electronic structure, exploiting the interference occuring between electronic wave function replicas produced by the train.

119. Morlens AS, Lopez-Martens R, Boyko O, Zeitoun P, Balcou P, et al. 2006. Design and characterization of extreme-UV broadband mirrors for attosecond science. *Opt. Lett.* 31:1558–60
120. Wonisch A, Neuhausler U, Kabachnik NM, Uphues T, Uiberacker M, et al. 2006. Design, fabrication, and analysis of chirped multilayer mirrors for reflection of extreme-UV attosecond pulses. *Appl. Opt.* 45:4147–56
121. Ghafur O, Kling M, Schultze M, Drescher M, Krausz F, Vrakking MJJ. 2007. A velocity map imaging detector for high repetition-rate low photon-flux experiments. In preparation
122. Ullrich J, Moshammer R, Dorn A, Dörner R, Schmidt LPH, Schmidt-Böcking H. 2003. Recoil-ion and electron momentum spectroscopy: reaction microscopes. *Rep. Prog. Phys.* 66:1463–545
123. Naumova NM, Nees JA, Sokolov IV, Hou B, Mourou GA. 2004. Relativistic generation of isolated attosecond pulses in a λ_3 focal volume. *Phys. Rev. Lett.* 92:063902
124. Ackermann W, Asova G, Ayvazyan V, Zaima A, Baboi N, et al. 2007. Operation of a free-electron laser from the extreme UV to the water window. *Nat. Photonics* 1:336–42
125. Zholents AA, Penn G. 2005. Obtaining attosecond X-ray pulses using a self-amplified spontaneous emission free electron laser. *Phys. Rev. Spec. Top. Accel. Beams* 8:050704
126. Zanghellini J, Kitzler M, Zhang Z, Brabec T. 2005. Multi-electron dynamics in strong laser fields. *J. Mod. Opt.* 52:479–88
127. Remacle F, Nest M, Levine RD. 2007. Laser steered ultrafast quantum dynamics of electrons in LiH. Submitted
128. Kono H, Sato Y, Tanaka N, Kato T, Nakai K, et al. 2004. Quantum mechanical study of electronic and nuclear dynamics of molecules in intense laser fields. *Chem. Phys.* 304:203–26
129. Marques MAL, Gross EKU. 2004. Time-dependent density functional theory. *Annu. Rev. Phys. Chem.* 55:427–55

RELATED RESOURCES

Online talks of the KITP Conference: Attosecond Science Workshop (July 31—September 15, 2006), **http://online.kitp.ucsb.edu/online/atto_c06/**

Attoworld, **http://www.attoworld.de**

Institute for Atomic and Molecular Physics, **http://www.amolf.nl**

Annual Review of
Physical Chemistry

Volume 59, 2008

Contents

Indexes

Errata

An online log of corrections to *Annual Review of Physical Chemistry* articles may be found at http://physchem.annualreviews.org/errata.shtml